https://ntrs.nasa.gov/search.jsp?R=19930087475 2020-06-17T09:07:14+00:00Z

SECURITY INFORMATION

CONFIDENTIAL

Copy 278
RM L52L26a

NACA

RESEARCH MEMORANDUM

EFFECTS OF ROUGHNESS AND REYNOLDS NUMBER ON THE NONLINEAR LIFT CHARACTERISTICS OF A WING WITH MODIFIED HEXAGONAL AIRFOIL SECTIONS

By Milton A. Schwartzberg

Langley Aeronautical Laboratory
Langley Field, Va.

CLASSIFICATION CHANGED TO UNCLASSIFIED

AUTHORITY J.W. CROWLEY DATE: 10-12-54

CHANGE NO. 2777 WHL

CLASSIFIED DOCUMENT

This material contains information affecting the National Defense of the United States within the meaning of the espionage laws, Title 18, U.S.C., Secs. 793 and 794, the transmission or revelation of which in any manner to an unauthorized person is prohibited by law.

NATIONAL ADVISORY COMMITTEE
FOR AERONAUTICS

WASHINGTON

February 9, 1953

CONFIDENTIAL

NATIONAL ADVISORY COMMITTEE FOR AERONAUTICS

RESEARCH MEMORANDUM

EFFECTS OF ROUGHNESS AND REYNOLDS NUMBER ON THE NONLINEAR LIFT CHARACTERISTICS OF A WING WITH MODIFIED HEXAGONAL AIRFOIL SECTIONS

By Milton A. Schwartzberg

SUMMARY

The lift characteristics of a wing with an aspect ratio of 4.364, a taper ratio of 0.41, zero sweep of the trailing edge, and modified hexagonal airfoil sections parallel to the air stream were investigated in the Langley low-turbulence pressure tunnel at Mach numbers from 0.379 to 0.896. Nonlinearities in the lift curves were obtained at small angles of attack for Reynolds numbers of the order of 1×10^6 at all test Mach numbers. Increasing the Reynolds numbers to 3×10^6 and 5×10^6 eliminated nearly all the observed nonlinearities. The addition of surface roughness to the test model at the lower Reynolds numbers also eliminated a large portion of the nonlinearities in the lift curves obtained for the smooth model. An explanation is offered of the boundary-layer phenomena probably responsible for the results obtained.

INTRODUCTION

Marginal directional stability has been exhibited at small angles of sideslip and low tail Reynolds numbers in tests of a complete airplane configuration employing a vertical tail of modified hexagonal chordwise sections. It was thought possible that low values of the tail lift-curve slope at small angles of attack might be responsible for the unsatisfactory directional stability of the airplane. Nonlinear lift characteristics, manifested by a decrease in lift-curve slope through a range of small positive and negative angles of attack, have been noted in previous airfoil and wing investigations at low Reynolds numbers, particularly with sharp-leading-edge airfoil sections (refs. 1 to 3, for example). These nonlinearities and the marginal directional stability previously mentioned have been found to be considerably improved at higher Reynolds numbers. The decisive effect of Reynolds number on the experimental results suggests that the controlling factors involved are

primarily boundary-layer phenomena. The present tests were conducted, therefore, to determine whether the effect of an increase in Reynolds number on the low-angle-of-attack lift characteristics of a wing with modified hexagonal chordwise sections could be duplicated at a low Reynolds number by changes in the wing surface condition.

SYMBOLS

b	wing span
c	wing local chord measured parallel to plane of symmetry
$\bar{c}$	wing mean aerodynamic chord, $\frac{2}{S}\int_0^{b/2} c^2 dy$
C_L	lift coefficient, L/qS
C_M	pitching-moment coefficient about $0.25\bar{c}$, $M_{\bar{c}/4}/qS\bar{c}$
L	lift
M	free-stream Mach number
$M_{\bar{c}/4}$	pitching moment about $0.25\bar{c}$
q	free-stream dynamic pressure, $\frac{1}{2}\rho V^2$
r	local fuselage radius
R	free-stream Reynolds number, $V\bar{c}/\nu$
R_c	radius of curvature
S	wing area
$\left(\frac{t}{c}\right)_{max}$	wing local maximum thickness ratio
V	free-stream velocity
x	longitudinal distance measured from nose of fuselage along model plane of symmetry

y	spanwise coordinate
α	angle of attack
ν	kinematic viscosity
ρ	free-stream mass density

MODEL AND TESTS

The tests were conducted in the Langley low-turbulence pressure tunnel in an atmosphere of Freon-12 gas through a Mach number range from 0.379 to 0.896. The test model is shown in figure 1.

The wing had an aspect ratio of 4.364, a taper ratio of 0.41, and zero sweep of the trailing edge. Figure 2 illustrates the nature of the wing sections and their variation across the span. The wing sections were of a symmetrical hexagonal form modified by rounding of the spanwise ridge lines to the radii shown in figure 2. The chordwise extent of the wing section maximum thickness varied along the span from 0.0c at the root to 0.25c at the 31.5-percent-semispan station to 0.11c at the tip chord. These chordwise extents of the maximum thickness do not correspond to the chordwise distances between the theoretical intersection lines (fig. 2) because of the rounding of the ridges at the surface intersections. The maximum thickness decreased from 0.08c at the root to 0.054c at the 31.5-percent-semispan station and remained constant at the latter value to the tip chord.

The body had a fineness ratio of 5.32 and a frontal area equal to 5 percent of the total wing area. The body coordinates are tabulated in figure 1.

A photograph of the test model is presented as figure 3, which also shows the conical fairing that housed the external-type strain-gage balance.

The variation of the test Reynolds number with the test Mach number is shown in figure 4 for the two values of free-stream stagnation pressure employed in the tests.

Lift and pitching moment were measured on the model in the smooth surface condition through both the low and high ranges of Reynolds number. The tests were then repeated with roughness elements on a $\frac{1}{8}$-inch-wide strip of adhesive agent that spanned both wing surfaces $\frac{1}{8}$ inch

ahead of the 30-percent-chord station. The roughness consisted of carborundum grains dispersed to occupy approximately 10 percent of the total adhesive-agent area. Average carborundum grain sizes of 0.005 inch and 0.011 inch were used in two successive series of tests.

All the data were converted to equivalent air data by the methods of reference 4. Corrections have been applied to the data to account for the tunnel blockage and induced upwash effects.

RESULTS

The results obtained for the smooth test model at Reynolds numbers of the order of 1×10^6 through a Mach number range from 0.379 to 0.896 are shown by the lift curves of figure 5. A decrease in the lift-curve slope is apparent at each Mach number in the range of angles of attack from -1° to 1°. Figure 6 depicts the results obtained on the smooth test model at increased Reynolds numbers of the order of 3×10^6 to 5×10^6. The nonlinear nature of the lift curves at the low Reynolds numbers has been almost completely eliminated at the higher Reynolds numbers. Some small nonlinearity can still be seen within a decreased angle-of-attack range.

Lift curves obtained at Reynolds numbers of the order of 1×10^6 with spanwise transition strips of approximately 0.005-inch grain size situated in the neighborhood of the 0.30c station on both wing surfaces are shown in figure 7. The presence of the roughness is seen to alleviate the nonlinearity of the lift curves as obtained on the smooth model at the same Reynolds numbers (fig. 5) to a considerable extent although not so markedly as did the increased Reynolds numbers. Lift curves obtained at the low Reynolds numbers with transition strips of approximately 0.011-inch grain size at the same chordwise station on the model surfaces were similar in all respects to those obtained with the smaller roughness particles. The model was also tested at the higher Reynolds numbers with transition strips of both roughness sizes situated successively at the same chordwise station without any noteworthy difference observed between these results and those obtained for the smooth model at the higher Reynolds numbers.

The test results are more graphically illustrated by the typical comparative curves of figure 8. The lift curves obtained with roughness on the model at the low Reynolds numbers form approximately a median between the lift curves obtained at low and high Reynolds numbers for the smooth model.

The variations with Mach number of the lift-curve slope of the test model as determined for angles of attack of 0° and 3° for the several test conditions are shown in figure 9. The theoretical lift-curve slope obtained from reference 5 for the present plan form is also included in figure 9. The lift-curve slopes for the smooth model at low Reynolds numbers at an angle of attack of 0° are considerably below the theoretical value throughout the subcritical Mach number range. The addition of roughness or an increase in Reynolds number increased the low-angle-of-attack lift-curve slope, with the increase in Reynolds number more effective than the roughness. The lift-curve slopes for the model at low Reynolds numbers at an angle of attack of 3° are higher than the theoretical values with no appreciable differences between the smooth and rough model conditions.

Pitching-moment data accumulated in the present tests are of questionable accuracy but may be used to indicate general trends with Mach number as well as the pronounced effects of roughness and Reynolds number. The variations with Mach number of the slopes of the pitching-moment curves $dC_M/d\alpha$ as determined for an angle of attack of 0° for several test conditions are shown in figure 10. The smooth model at low Reynolds numbers was unstable through the subcritical Mach number range. Both roughness and increased Reynolds numbers had approximately the same stabilizing effect on the model throughout the Mach number range of the tests.

DISCUSSION

A possible explanation of the test results obtained at subcritical speeds is presented in the following discussion in terms of the boundary-layer flow phenomena involved. Although no detailed boundary-layer measurements have been made in order to corroborate this explanation, confirmation of the various flow concepts discussed herein can be found in many sources.

There are two factors which may be considered to contribute to the decreased lift-curve slope of the smooth model at small angles of attack and low Reynolds numbers. These are the presence of a localized region of boundary-layer separation at the leading edge and the effects of this region and the differences between the upper- and lower-surface pressure distributions on the respective boundary-layer thicknesses. Many investigations have indicated the formation of a separation "bubble" shortly after the beginning of an adverse pressure gradient. The boundary-layer flow following such a bubble is turbulent. Both the bubble size and the size of the subsequent turbulent boundary layer increase with angle of attack. At a small positive angle of attack, a more favorable pressure gradient of greater chordwise extent exists on the lower surface of an airfoil than on the upper surface and the adverse pressure gradient

toward the rear on the lower surface is less severe than on the upper. Pressure distributions of reference 3 on similar airfoils substantiate these observations. The combined effects of a separation bubble on the upper surface and the differences in pressure distributions on the two surfaces results in a more rapid growth of the turbulent boundary layer in the region of the model trailing edge on the upper surface than on the lower surface as the angle of attack is increased from zero. The rate of displacement of the flow outside the boundary layer in the region of the model trailing edge with increasing angle of attack, therefore, is greater on the upper surface than on the lower surface with a resultant decreased lift-curve slope as compared to the theoretical value for a potential flow. This decrease in lift-curve slope through an angle of attack of 0° is shown in figure 9 for the smooth model at low Reynolds numbers by comparison with the theoretically predicted values from reference 5.

Similar results have been observed for airfoils with beveled-trailing-edge ailerons. The beveled-trailing-edge aileron, at an aileron deflection of 0° and small angle of attack, has been compared to an upwardly deflected trailing-edge tab (ref. 6) in creating a negative load at the trailing edge for the reduction of control-surface hinge moments. For the present model, the increasing difference in size between the upper- and lower-surface trailing-edge boundary layers with increasing angle of attack produces an effect similar to a continuous increase in upward tab deflection with increasing angle of attack, that is, an increase in negative load increment at the model trailing edge. This explanation is further substantiated by the positive values of $dC_M/d\alpha$ obtained for the smooth model at low Reynolds numbers (fig. 10).

The increase in size of the separation bubble at the leading edge of an airfoil with angle of attack is thought to effect an increase in lift-curve slope of the airfoil in the same manner as a continuous increase in airfoil camber. This effect, which is very slight at low angles of attack, becomes sufficiently pronounced with increasing angle of attack to outweigh the influence of the asymmetry in the upper- and lower-surface boundary layers near the trailing edge and increases the lift-curve slope as shown by the test results in figure 5. It is shown in figure 9 that, at an angle of attack of 3°, the rate of increase of the camber effect of the separation bubble with angle of attack is great enough to result in a larger value of the lift-curve slope than that predicted by the theory of reference 5.

The changes in the lift curves, with an increase in free-stream Reynolds number (figs. 5, 6, and 8), are brought about by a twofold effect of the increased Reynolds number on the boundary-layer thickness. First, increased Reynolds number reduces the size of the upper-surface separation bubble with a resultant smaller immediate increase in upper-surface

boundary-layer thickness in the region of the bubble (ref. 7) and a consequent reduced trailing-edge boundary-layer thickness. Second, an increase in Reynolds number thins the boundary layers on both model surfaces, so that the rate of change with angle of attack of the difference between the upper- and lower-surface trailing-edge boundary-layer thicknesses decreases with increasing Reynolds number. The net effect of an increase in Reynolds number, therefore, is an increase in lift-curve slope at small angles of attack as shown by the test results.

The transition strips on the model at low Reynolds numbers partially accomplished the same results as an increase in Reynolds number at the low angles of attack but through a different effect on the model boundary layer. The transition strips assured early transition of the boundary layer on the model lower surface and, therefore, a thicker trailing-edge boundary layer on the lower surface than for the smooth model condition. This was again a means of decreasing the rate of change with angle of attack of the difference between the upper- and lower-surface trailing-edge boundary-layer thicknesses and thus resulted in an increased lift-curve slope.

CONCLUDING REMARKS

Experimental results, through a Mach number range from 0.379 to 0.896, on a wing-fuselage model with a straight trailing edge, a taper ratio of 0.41, and symmetrical modified hexagonal airfoil sections parallel to the air stream indicated decreased lift-curve slopes at test Reynolds numbers of the order of 1×10^6 for angles of attack from -1° to 1°. The lift curves became steeper and very nearly linear for increased test Reynolds numbers of 3×10^6 to 5×10^6. A large portion of the same effect as obtained with the increased Reynolds numbers was also achieved at the low Reynolds numbers with roughness added in the neighborhood of the spanwise ridge line near the 30-percent-chord station. An explanation of the boundary-layer phenomena probably involved in determining the nature of the test results is presented.

Langley Aeronautical Laboratory,
National Advisory Committee for Aeronautics,
Langley Field, Va.

REFERENCES

1. Underwood, William J., and Nuber, Robert J.: Two-Dimensional Wind-Tunnel Investigation at High Reynolds Numbers of Two Symmetrical Circular-Arc Airfoil Sections With High-Lift Devices. NACA RM L6K22, 1947.

2. Neely, Robert H., and Koven, William: Low-Speed Characteristics in Pitch of a 42° Sweptback Wing With Aspect Ratio 3.9 and Circular-Arc Airfoil Sections. NACA RM L7E23, 1947.

3. Lindsey, W. F., Daley, Bernard N., and Humphreys, Milton D.: The Flow and Force Characteristics of Supersonic Airfoils at High Subsonic Speeds. NACA TN 1211, 1947.

4. Von Doenhoff, Albert E., and Braslow, Albert L.: Studies of the Use of Freon-12 As a Testing Medium in the Langley Low-Turbulence Pressure Tunnel. NACA RM L51I11, 1951.

5. DeYoung, John, and Harper, Charles W.: Theoretical Symmetric Span Loading at Subsonic Speeds for Wings Having Arbitrary Plan Form. NACA Rep. 921, 1948.

6. Jones, Robert T., and Ames, Milton B., Jr.: Wind-Tunnel Investigation of Control-Surface Characteristics. V - The Use of a Beveled Trailing Edge To Reduce the Hinge Moment of a Control Surface. NACA WRL-464, 1942. (Formerly NACA ARR, Mar. 1942.)

7. Bursnall, William J., and Loftin, Laurence K., Jr.: Experimental Investigation of Localized Regions of Laminar-Boundary-Layer Separation. NACA TN 2338, 1951.

Body Coordinates

x	r
1/2	.31
1	.48
2	.77
3	1.00
4	1.215
5	1.38
6	1.50
7	1.59
8	1.605
9	1.595
10	1.54
11	1.485
12	1.395
13	1.295
14	1.175
15	1.06
16	1.01
17 1/16	1.00

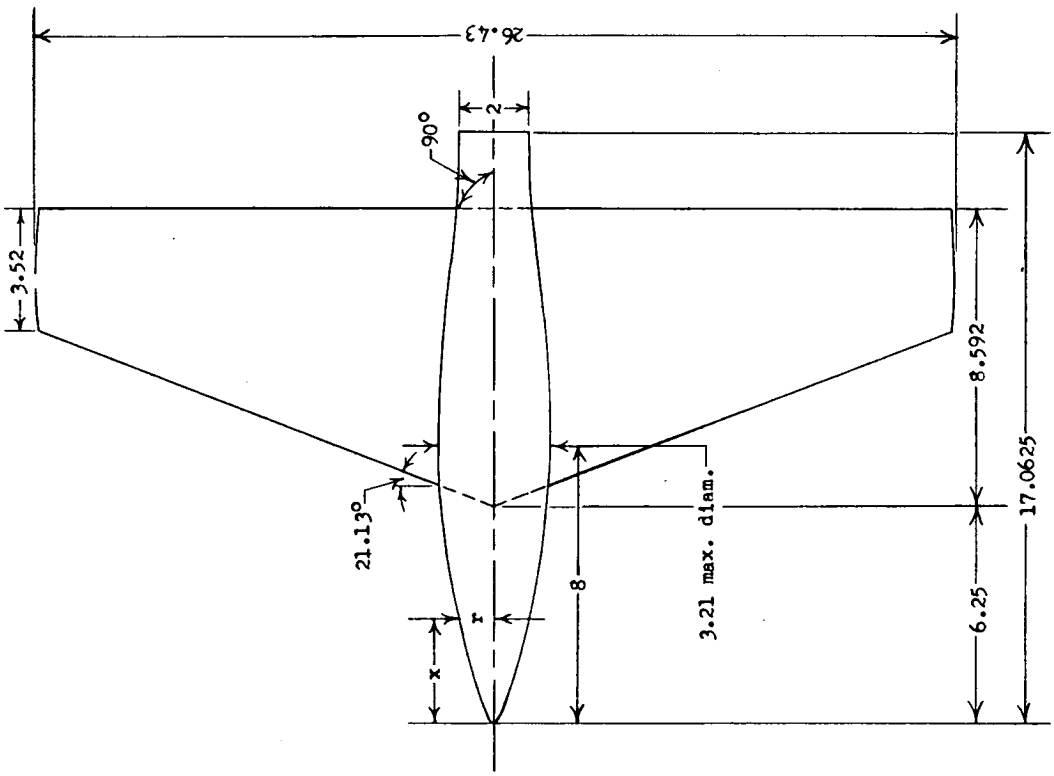

Figure 1.- Test model configuration. Dimensions are in inches except as noted.

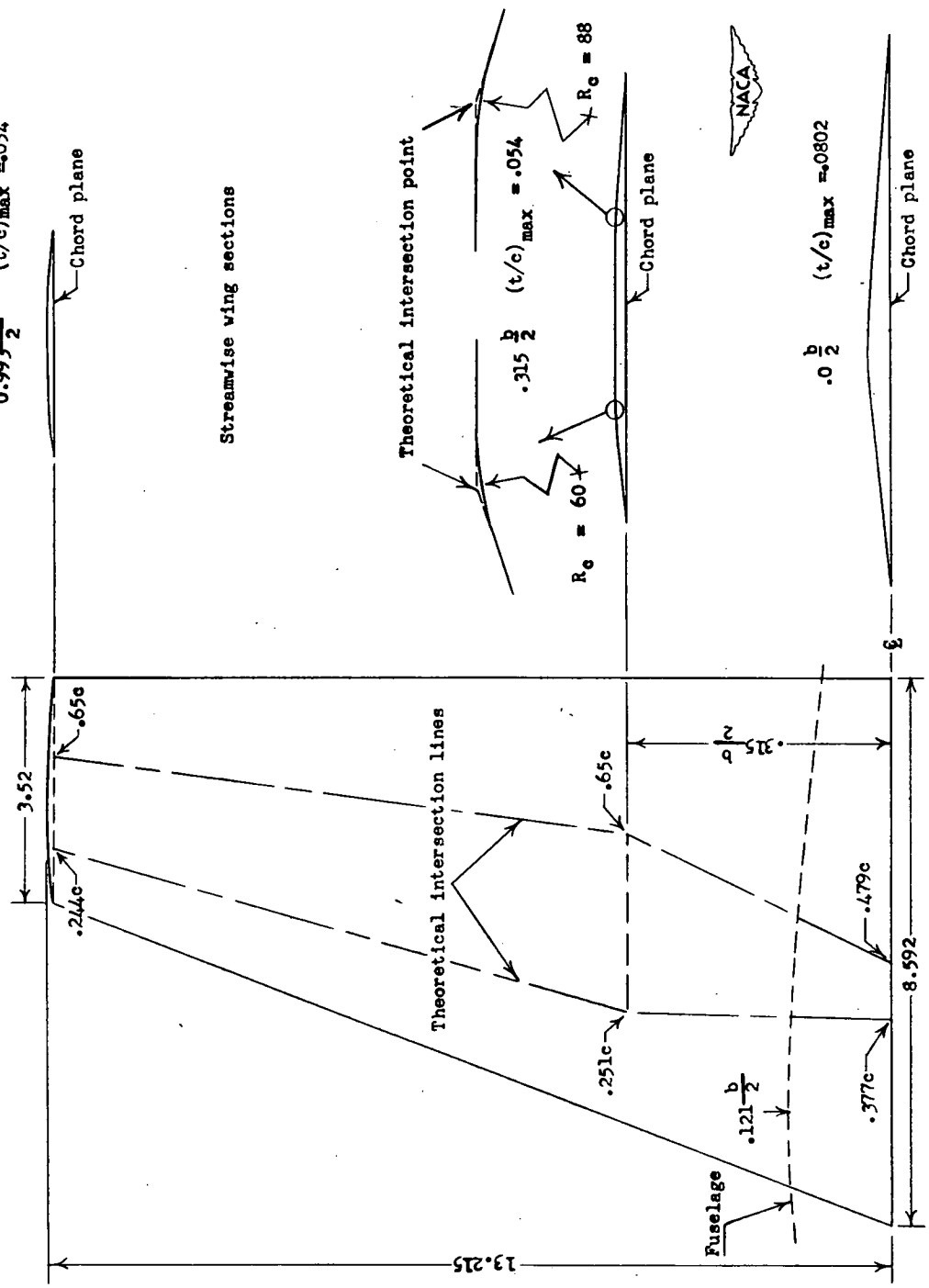

Figure 2.- Wing plan form and streamwise sections. All dimensions are in inches.

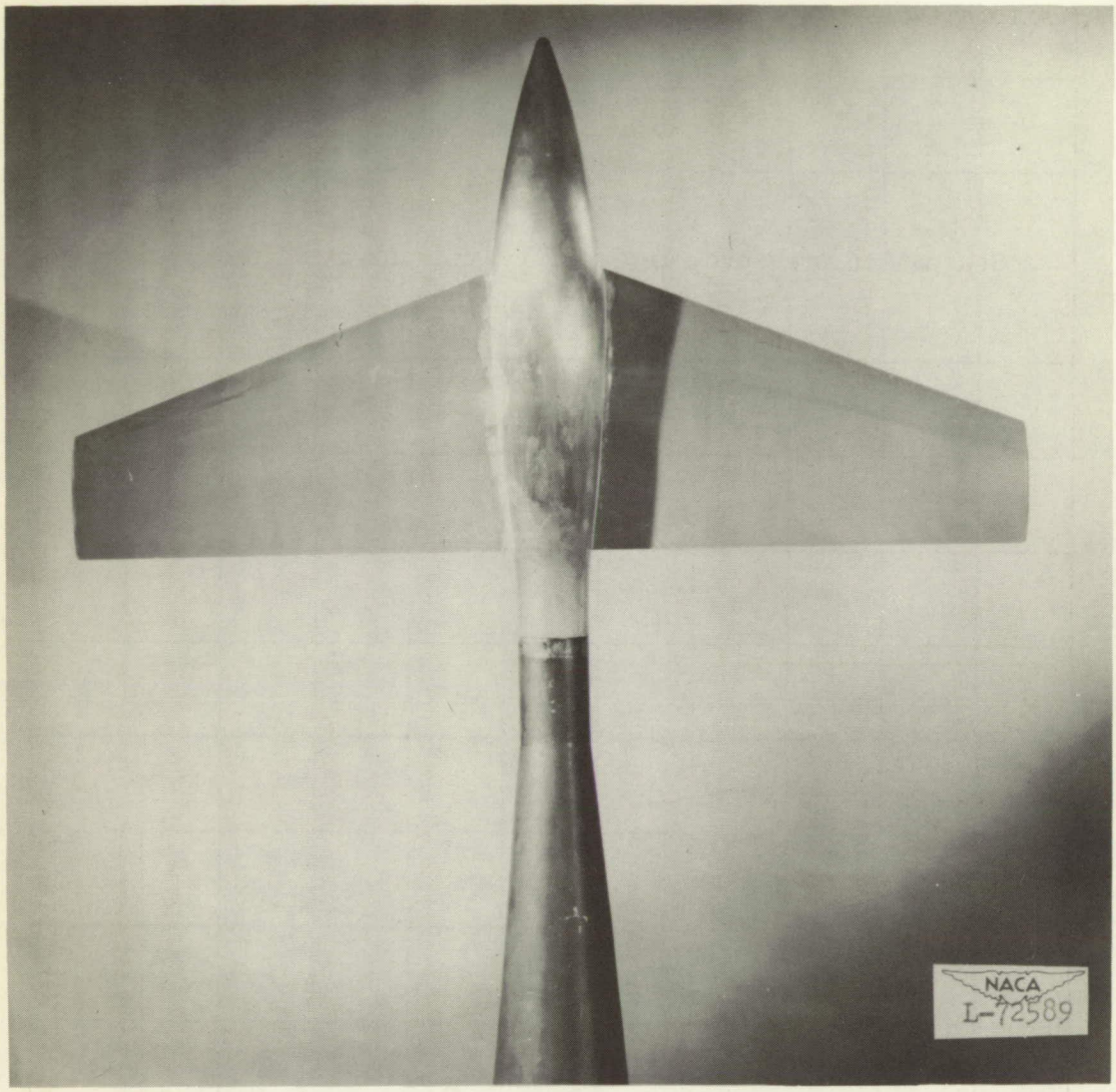

Figure 3.- Test model and conical balance fairing.

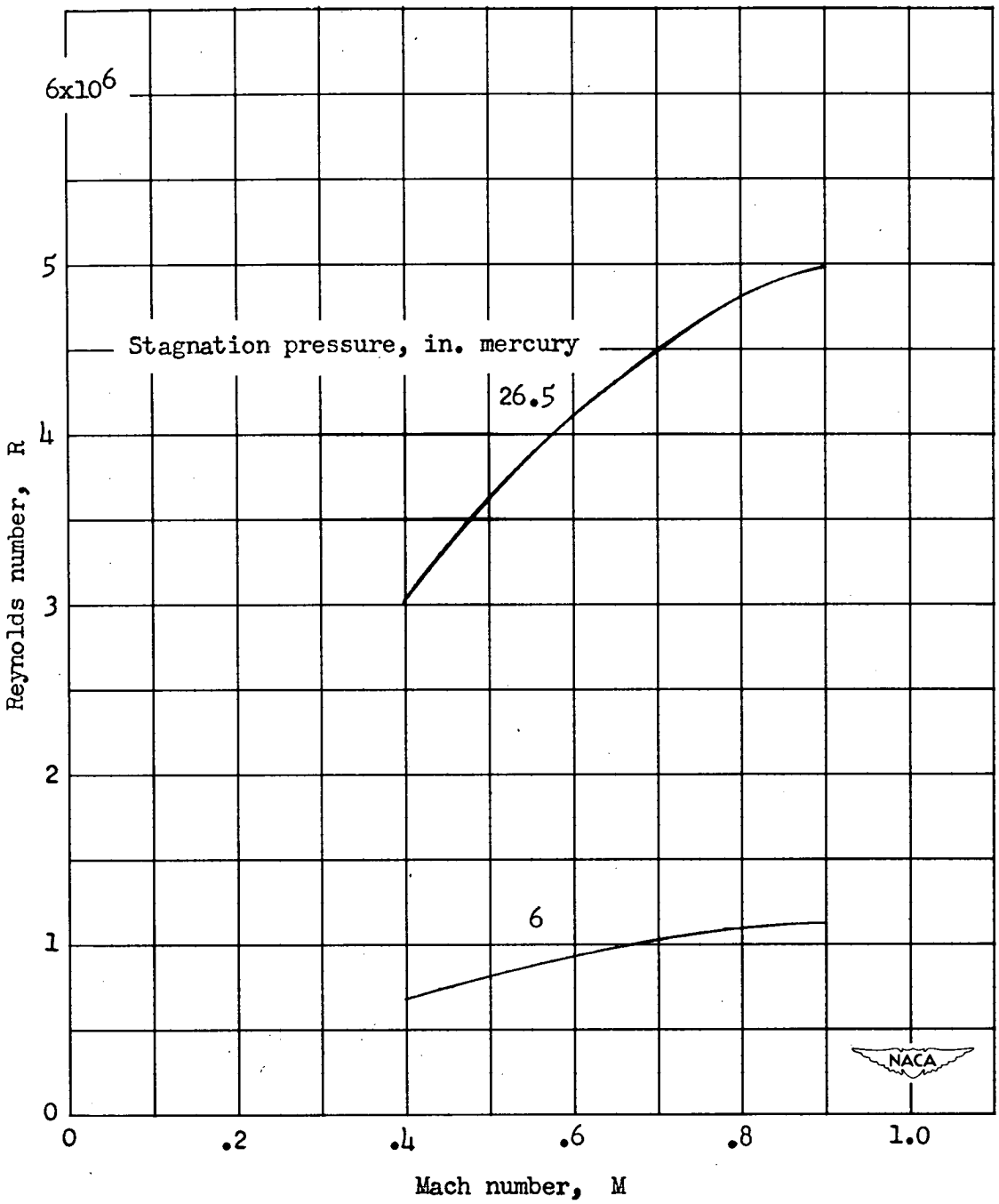

Figure 4.- Variation of test Reynolds number with Mach number.

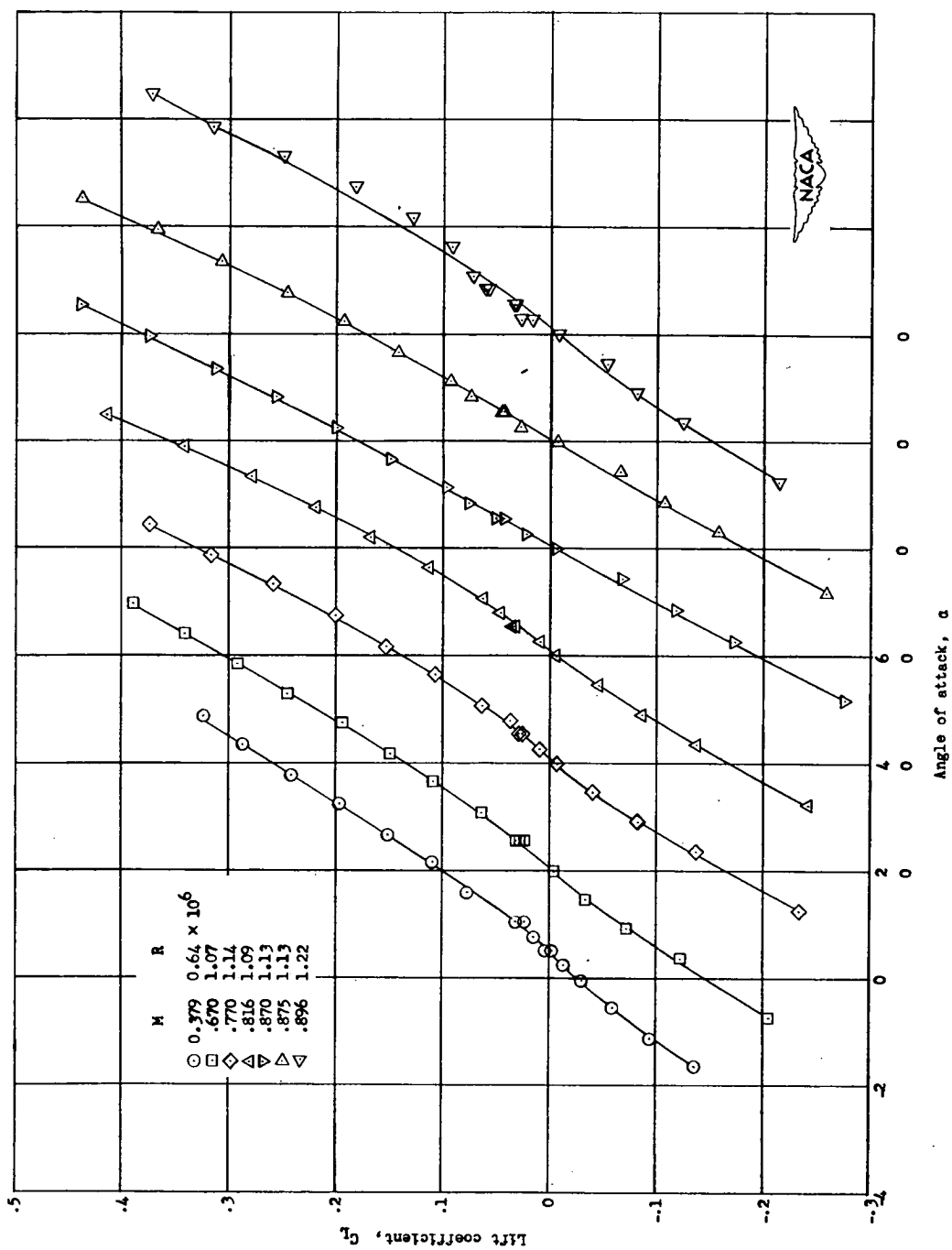

Figure 5.- Lift coefficients for smooth test model at low Reynolds numbers.

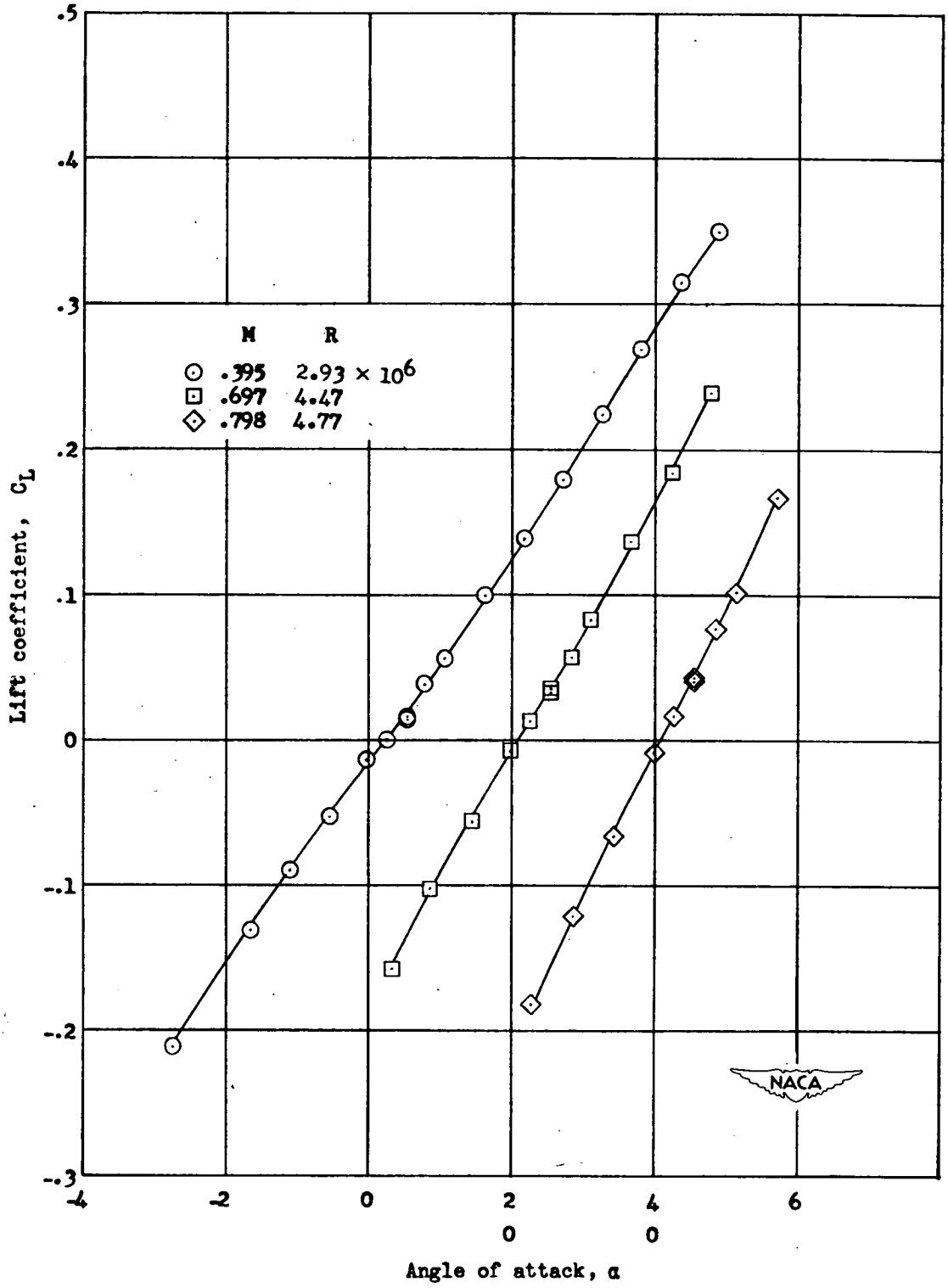

Figure 6.- Lift coefficients for smooth test model at high Reynolds numbers.

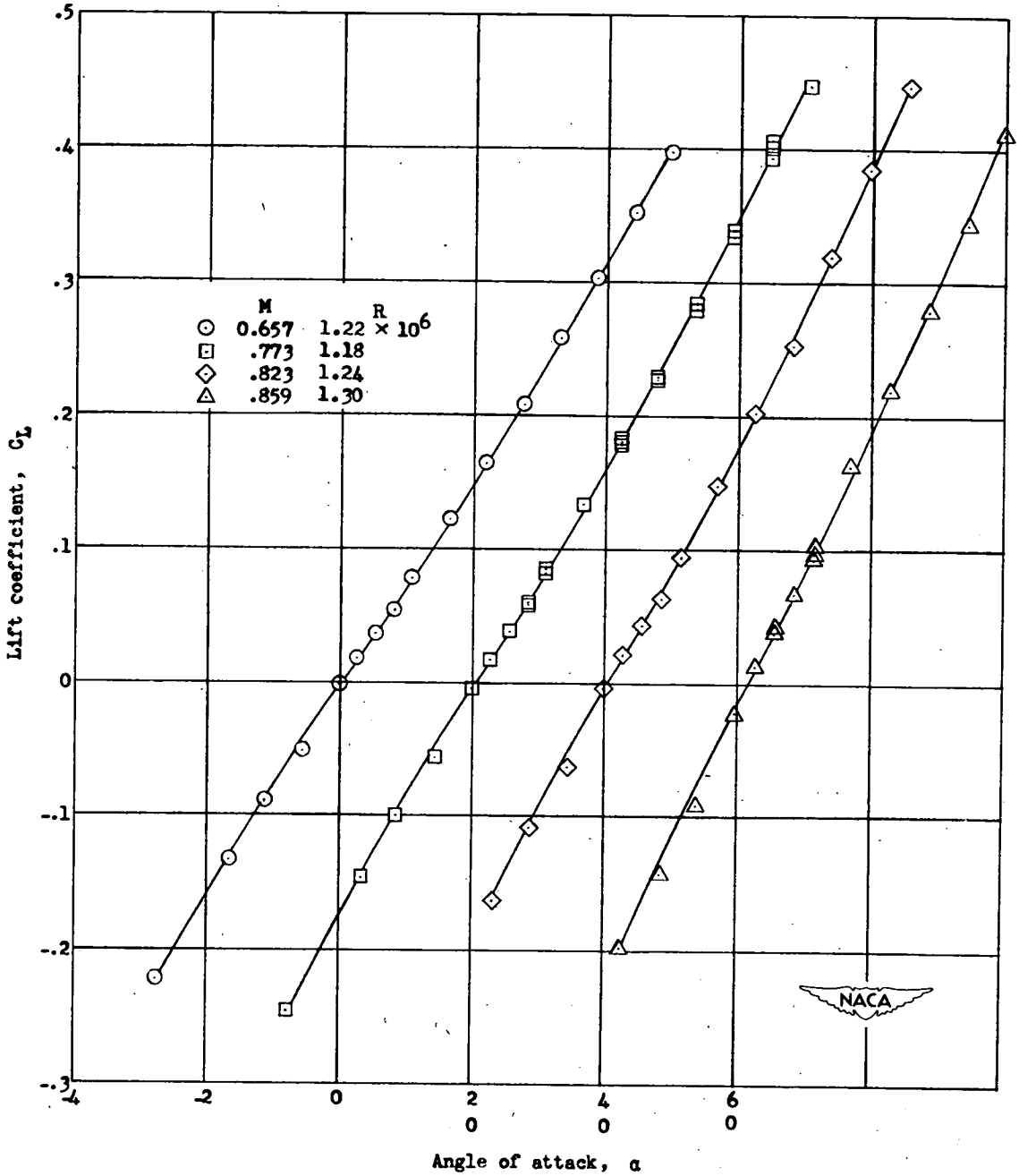

Figure 7.- Lift coefficients for test model at low Reynolds numbers with surface roughness in the neighborhood of the 0.30c station.

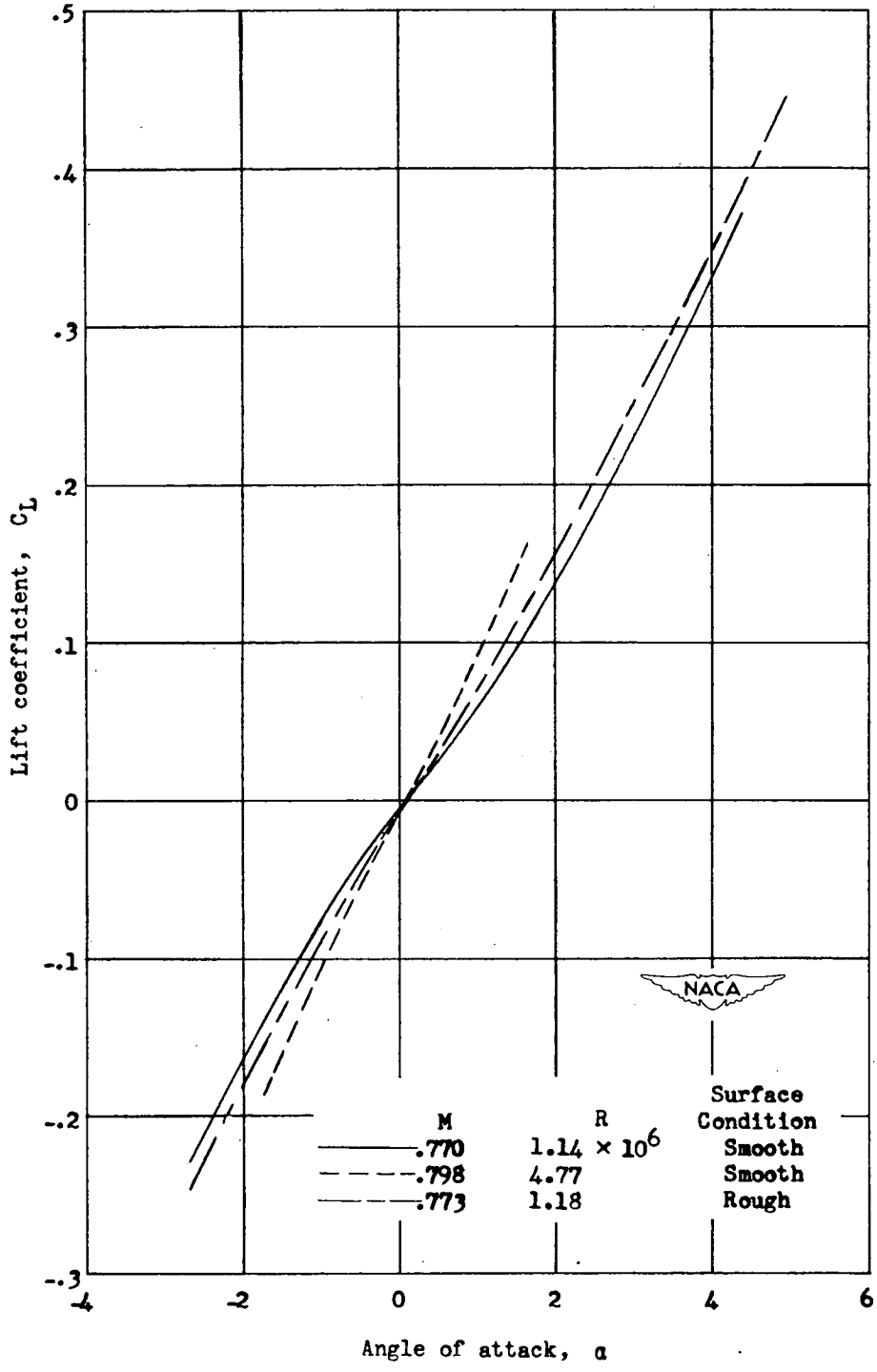

Figure 8.- Comparison of lift coefficients for smooth test model at high and low Reynolds numbers with lift coefficients for model at a low Reynolds number with surface roughness in the neighborhood of the 0.30c station.

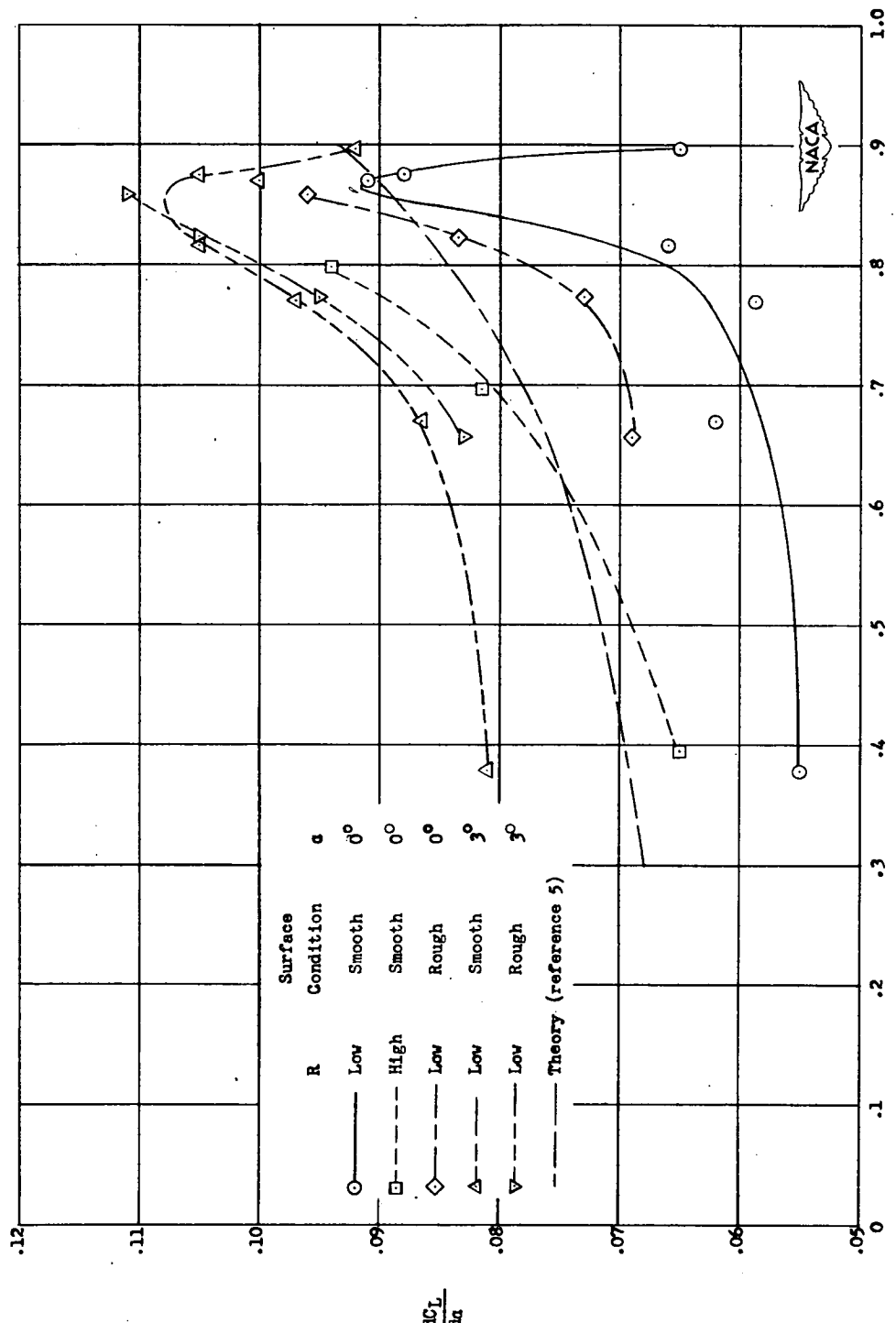

Figure 9.- Variation of lift-curve slopes at angles of attack of 0° and 3° with Mach number for several model conditions and a comparison with the theoretical lift-curve slopes determined from reference 5.

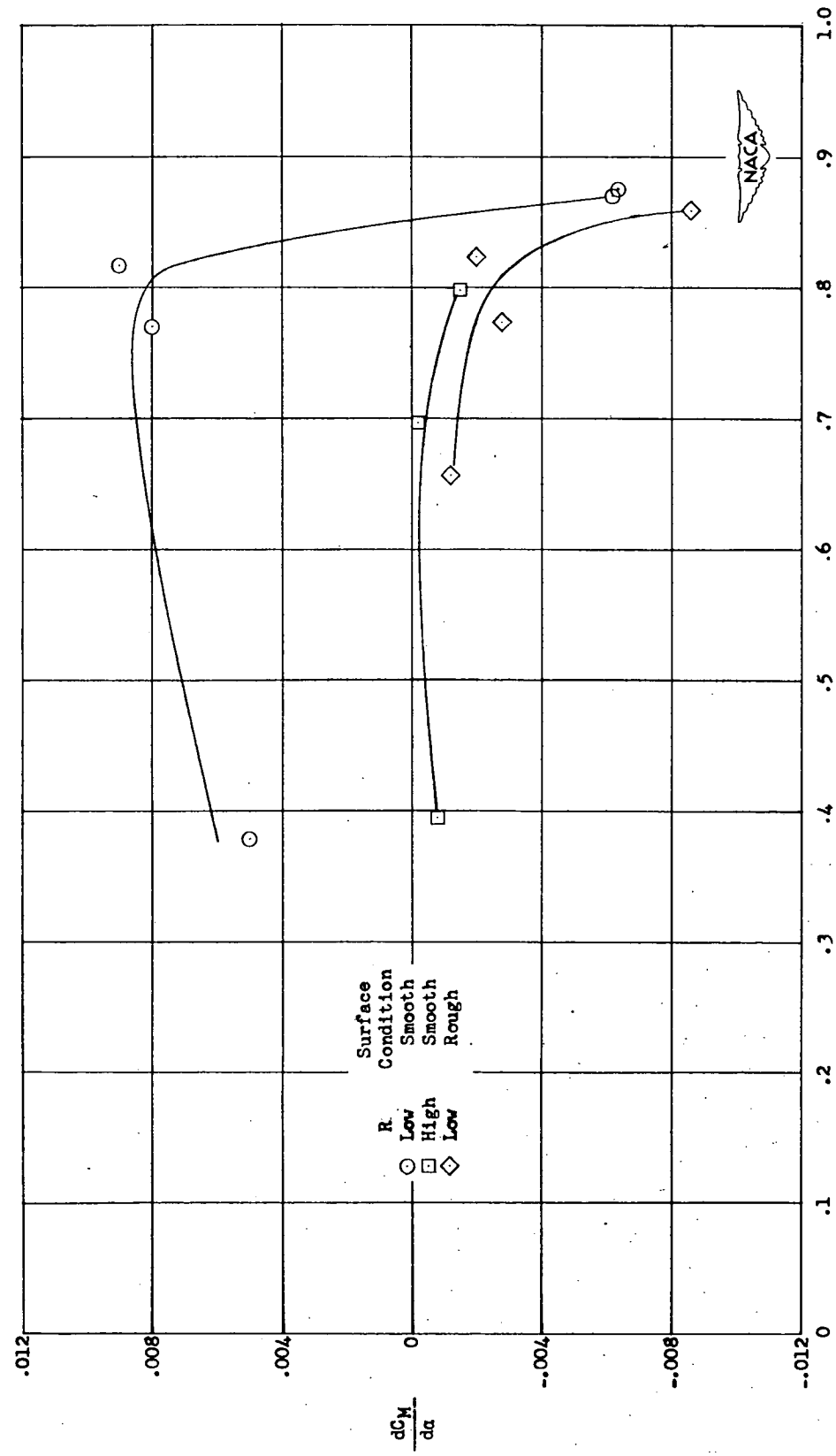

Figure 10.- Variation of slope of pitching-moment curves at angle of attack of 0° with Mach number for several model conditions.

NACA-Langley - 2-9-53 - 325